Science of the Total Environment 829 (2022) 154638

Contents lists available at ScienceDirect

Science of the Total Environment

journal homepage: www.elsevier.com/locate/scitotenv

Zinc nanoparticles: Mode of action and efficacy against boscalid-resistant *Alternaria alternata* isolates

Anastasios A. Malandrakis [a,*], Nektarios Kavroulakis [b], Constantinos V. Chrysikopoulos [a]

[a] School of Environmental Engineering, Technical University of Crete, 73100 Chania, Greece
[b] Hellenic Agricultural Organization "Demeter", Institute for Olive Tree, Subtropical Plants and Viticulture, Agrokipio-Souda, 73164 Chania, Greece

HIGHLIGHTS

- ZnO-NPs were used to combat boscalid resistance in *A. alternata*.
- A synergistic effect was observed between ZnO-NPs and boscalid or fluazinam.
- Zn^{+2} release or ROS production accounts for the ZnO-NPs fungitoxic action.
- Ion homeostasis is probably involved in the superior ZnO-NPs toxic activity.

GRAPHICAL ABSTRACT

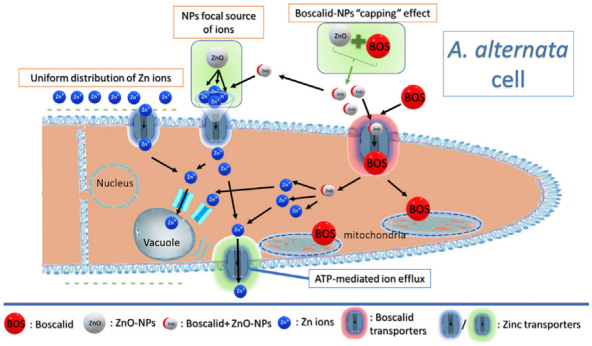

ARTICLE INFO

Article history:
Received 25 January 2022
Received in revised form 1 March 2022
Accepted 14 March 2022
Available online 18 March 2022

Editor: Damia Barcelo

Keywords:
Carboxamides
Nanofungicides
Plant pathogens
ZnO-NPs
Synergism

ABSTRACT

The antifungal potential of ZnO-NPs against *Alternaria alternata* isolates with reduced sensitivity to the succinate dehydrogenase inhibitor (SDHI) boscalid, resulting from target site modifications, was evaluated *in vitro* and *in vivo*. ZnO-NPs could effectively inhibit mycelial growth in a dose-dependent way in both boscalid (BOSC) sensitive (BOSC-S) and resistant (BOSC-R) isolates. The fungitoxic effect of ZnO-NPs against the pathogen was significantly enhanced when combined with boscalid compared to the individual treatments in all phenotype cases (BOSC-S/R) both *in vitro* and *in vivo*. Fungitoxic effect of ZnO-NPs could be, at least partly, attributed to zinc ion release as indicated by the positive correlation between sensitivities to the nanoparticles and their ionic counterpart $ZnSO_4$ and the alleviation of the ZnO-NPs fungitoxic action in the presence of the strong chelating agent EDTA. The superior effectiveness of ZnO-NPs against *A. alternata*, compared to $ZnSO_4$, could be due to nanoparticle properties interfering with cellular ion homeostasis mechanisms. The observed additive action of the oxidative phosphorylation-uncoupler fluazinam (FM) against all phenotypes indicates a possible role of ATP-dependent ion efflux mechanism in the mode of action of ZnO-NPs. A potential role of ROS production in the fungitoxic action of ZnO-NPs was evident by the additive/synergistic action of salicylhydroxamate (SHAM), which blocks the alternative oxidase antioxidant action. Mixture of ZnO-NPs and boscalid, resulting in a "capping" effect for the nanoparticles and significantly reducing their mean size, probably accounted for the synergistic effect of the mixture against both sensitive and resistant *A. alternata* isolates. Summarizing, results indicated that ZnO-NPs can be effectively used against *A. alternata* both alone or in combination with boscalid, providing an effective tool for combating SDHI-resistance and reducing the environmental fingerprint of synthetic fungicides.

1. Introduction

All alternative measures to combat plant diseases considered, chemical control utilizing protective or systemic synthetic fungicides still remains the

* Corresponding author.
E-mail address: tasmal@aua.gr (A.A. Malandrakis).

http://dx.doi.org/10.1016/j.scitotenv.2022.154638

most efficient and economically feasible disease management strategy so far, ensuring food sustainability and safety (Pandey et al., 2018; Malandrakis et al., 2018). Nevertheless, certain drawbacks of conventional fungicides such as side effects to non-target organisms and environmental pollution, especially aquifer contamination, have caused the withdrawal of a great number of fungicide active ingredients enforced by implementation of strict EU regulations (Malandrakis et al., 2021a, 2021b). This fact, in combination with the compromise of fungicide efficacy due to the emergence of fungicide-resistant pathogens, underline the necessity for alternative disease control measures capable of reducing disease incidence and, at the same time, mitigating environmental risks. Nanofungicides, containing nanoparticles (NPs) as active ingredients, are promising environmentally compatible fungicide alternatives due to their unique properties that include high antifungal effectiveness, enhanced residual action, and drug delivery and low resistance risk (Pandey et al., 2018; Kah et al., 2018; Sun et al., 2018). Zinc oxide NPs have a number of advantages including: low cost, increased stability in extreme conditions compared to their bulk counterparts, and substantial antimicrobial activity at low concentrations while being relatively safe to humans (Król et al., 2017; Sardella et al., 2017; Malandrakis et al., 2019; Sun et al., 2018). The fungitoxic potential of ZnO-NPs against fungal plant pathogens including *Fusarium* sp., *Sclerotinia homoeocarpa*, *Botrytis cinerea*, *Aspergillus niger*, *Penicillium expansum*, and *Rhizopus stolonifer* has been evaluated in a number of studies (Li et al., 2017; Król et al., 2017; Ashajyothi et al., 2016; Sardella et al., 2017). Several biochemical mechanisms responsible for their mycotoxic mode of action have been proposed, even though further studies are needed to acquire conclusive evidence in order to elucidate/validate these potential mechanisms (Sardella et al., 2017). DNA recombination, membrane/transmembrane transport, protein synthesis, ion homeostasis, and ROS generation/induction of oxidative stress are some of the proposed physiological processes that ZnO-NPs interfere with causing the toxic action against plant pathogens (Márquez et al., 2018; Rai et al., 2017; Khan et al., 2016; Malandrakis et al., 2019).

Alternaria alternata is a cosmopolitan fungal pathogen with a wide range of hosts causing economically significant yield losses in Cucurbitaceae, Brassicaceae and Solanaceae vegetables (Strandberg, 1992). Symptom severity depends on weather conditions, host and cultivar susceptibility, and pathogen pathotype; which vary from preharvest leaf blight, brown leaf spot, and stem canker to postharvest fruit rot (Morris et al., 2000; Strandberg, 1992). On tomato plants, the pathogen is mostly responsible for post-harvest damage of ripe tomato, especially affecting the tomato processing industry (Morris et al., 2000; Davis et al., 1997). On top of that, food safety issues arise from the ability of *A. alternata* to produce a number of mycotoxins (secondary metabolites that exert genotoxic, mutagenic or even acute toxic effects on humans) including tenuazonic acid (TeA), alternariol (AOH), and alternariol monomethyl ether (AME). This highlights the importance of effective control of the fungus (Logrieco et al., 2009).

Chemical control represents the main method for reducing the incidence of *A. alternata* utilizing both protective and systemic fungicides such as: demethylation inhibitors (DMIs), succinate dehydrogenase inhibitors (SDHIs), and quinone outside inhibitors (QoIs) (Sierotzki and Scalliet, 2013; Malandrakis et al., 2018). The SDHI, carboxamide boscalid is a very effective fungicide used against a wide range of plant pathogens including *A. alternata* (Malandrakis et al., 2018; Xiao and Boal, 2009; Avenot and Michailides, 2015). SDHIs target complex II of the respiration pathway by specifically binding with the succinate dehydrogenase enzyme blocking the electron transport chain and eventually resulting in cell death due to ATP starvation (Bartlett et al., 2002; Sierotzki and Scalliet, 2013). Unfortunately, due to the intensity of usage and their site specific mode of action, efficacy of these fungicides has been compromised due to the emergence of SDHI-resistant strains (Avenot et al., 2008; Veloukas et al., 2013; Avenot and Michailides, 2015; Fan et al., 2015; Malandrakis et al., 2017). Isolates of *A. alternata* resistant to SDHIs bearing mutations in 3 out of 4 SDH subunits were reported shortly after their introduction (Avenot and Michailides, 2015; Fan et al., 2015). Specifically, several substitutions in positions 277 of the *sdh*B subunit, 134 and 135 of the *sdh*C, and 47, 123 or 133 of the *sdh*D subunits of the SDH enzyme were associated with resistance to SDHIs in *A. alternata* (Sierotzki and Scalliet, 2013; Sang and Lee, 2020).

A novel, recently proposed, environmentally compatible countermeasure against drug/fungicide resistance concerns the use of metal nanoparticles alone or in combination with conventional drugs (Malandrakis et al., 2019, 2020a, 2020b, 2021b). Ag-NPs, ZnO-NP, and Fe-NPs have been reported to be effective (alone or in combination with antibiotics) against drug-resistant pathogenic bacteria including *Proteus mirabilis*, *Klebsiella pneumonia*, *Pseudomonas aeruginosa*, *Escherichia coli*, *Enterococcus faecalis*, and *Staphylococcus aureus* (Punjabi et al., 2018; Gabrielyan et al., 2019; Nejabatdoust et al., 2019; Paralikar et al., 2019). Furthermore, Ag-NPs, Cu-NPs, and ZnO-NPs used individually, or in combination with conventional fungicides, have also been reported to be effective against fungicide resistant fungal pathogens in a limited number of cases (Malandrakis et al., 2020a, 2020b, 2021a, 2021b; Huang et al., 2018; Jamdagni et al., 2018; Xue et al., 2014).

Under this light, this study aimed to: (a) evaluate the effectiveness of ZnO-NPs against sensitive and boscalid resistant *A. alternata* isolates, (b) investigate the potential of ZnO-NPs used in combinations with fungicides against sensitive/resistant *A. alternata* phenotypes both *in vitro* and on fruit, and (c) elucidate mechanisms underlying the mode of fungitoxic action of ZnO-NPs, and the synergy observed between ZnO-NPs and boscalid.

2. Materials and methods

2.1. Nanoparticles, fungicides and reagents

Zinc oxide nanoparticles [ZnO-NPs] (<100 nm particle size), zinc sulphate [$ZnSO_4$], ethylenediaminetetraacetic acid (EDTA) and salicylhydroxamate [SHAM], were purchased from Sigma Aldrich, MO, USA. Commercial fungicides containing active ingredients boscalid (Cantus 50 WG), fluazinam (Azzuro 50 SC), mancozeb (Trimanoc 75 WG) and Cu $(OH)_2$ (Copperblau-N 50 WP), were purchased from their respective manufacturers. Analytical grade active ingredients of remaining fungicides: tebuconazole and fenhexamid were supplied by Bayer CropScience AG (Leverkusen, Germany), pyraclostrobin and boscalid by BASF AG (Limburgerhof, Germany) and fludioxonil by Syngenta Crop Protection AG (Basle, Switzerland). All analytical grade stock solutions contained ethanol as a solvent in except for boscalid, and pyraclostrobin which were dispersed in methanol. In *in vitro* bioassays, active ingredients were added aseptically to sterilized growth medium prior to inoculation. Antifungal agent concentrations were prepared by adding appropriate quantities of the active ingredients making sure that the solvent never exceeded 1% (v:v) of the total volume. An appropriate volume of solvent was also added in the control treatments. Stock solutions of nanoparticles and commercial fungicides were prepared in distilled-sterilized water. In order to deter particle aggregation, nanoparticle suspensions were sonicated for 30 min using a Transonic 420 (Elma, Germany) sonicator prior to their incorporation in growth media. Zeta potential and hydrodynamic diameter measurements for the ZnO-NPs were measured in triplicate with a Zetasizer (Nano ZS90, Malvern Instruments, Southborough, MA).

2.2. Fungal isolates and culture conditions

Alternaria alternata isolates originated from infected tomato fruits collected from greenhouses located in Crete (southern Greece) during a survey conducted in 2020. Most greenhouses of collection had a prior history of frequent spaying with SDHIs (boscalid and fluopyram) and QoIs (pyraclostrobin, famoxadone) for at least 2 years. Conidia from infected fruit were scrapped using a sterilized needle under aseptic conditions, transferred in glass tubes containing sterilized water and plated on acidified PDA medium (containing 1 mL/L of lactic acid) in order to acquire single spore isolates and avoid bacterial infections. Single spore isolates were

identified to be *A. alternata* by morphological examination under a microscope, a fact subsequently validated by sequencing of the *sdh* gene subunits evaluated in this study. Ten isolates were selected for further assessment. Isolates used in fungitoxicity assays were kept on Potato Dextrose Agar (PDA) medium in growth chambers at 25 °C with 14 h day^{-1} light and 70% RH. Once every two months, isolates were transferred in PDA-containing glass tubes and stored at 4 °C in the dark for long-term storage.

2.3. In vitro bioassays

2.3.1. Sensitivity of A. alternata to ZnO-NPs and selected fungicides

The potential of zinc oxide NPs to control sensitive and fungicide-resistant *A. alternata* isolates, was evaluated by fungitoxicity tests *in vitro* utilizing the poison agar assay. Fungitoxicity was expressed as percent relative inhibition of isolates grown on PDA (except in the cases of treatments containing fluopyram and boscalid where water agar was used) amended with appropriate concentrations of the antifungal active ingredients. In order to assess the sensitivity of *A. alternata* isolates to fungicides, discriminatory concentrations equal to mean EC_{50} values (effective concentration causing 50% inhibition of mycelial growth) reported previously were used in the *in vitro* bioassays. Specifically, concentrations used were: 500 μg/mL for $Cu(OH)_2$, 0.05 μg/mL for fluazinam, 0.2 μg/mL for fludioxonil, 2 μg/mL for tebuconazole and 2.5 μg/mL for boscalid (Avenot and Michailides, 2015; Kalamarakis et al., 2000; Malandrakis et al., 2019; Markoglou et al., 2006). Sensitivity of *A. alternata* to ZnO-NPs was evaluated by applying concentrations of 10, 25, 50, 100, 250, 500 and 1000 μg/mL ZnO-NPs in order to obtain fungitoxicity-curves and calculate a mean EC_{50} value. EC_{50} values and respective resistance factors (Rf: EC_{50} of the resistant isolate over mean EC_{50} of sensitive isolates) of isolates with reduced sensitivity to boscalid were calculated by subjecting them to additional fungicide doses. Specifically, concentrations of 0, 0.1, 1, 2.5, 5, 10, 50, 100 and 150 μg/mL boscalid and 0, 0.01, 0.05, 1, 2.5, 5, 10 μg/mL fluopyram were used to obtain fungitoxicity-curves for *A. alternata* SDHI-resistant isolates. All fungicide concentrations were applied in triplicate. Growth media treated with antifungal agents or not (control) were inoculated with a 5-mm mycelial plug cut from the edge of a 4-day old colony of each isolate placed the center of each plate. Cultures were then incubated in a growth chamber at 25 °C with 70% RH in the dark for 4 days. The following formula: 100 − (mean diameter of the colony on the fungicide-treated plates divided by the mean diameter of the untreated control) × 100 was used to calculate percent inhibition rates. Tests were repeated twice for each isolate and antifungal agent concentration.

2.3.2. Synergy between ZnO-NPs and antifungal agents

Potential synergy activity of ZnO-NPs or their bulk/ionic counterpart $ZnSO_4$ when applied in mixtures with fungicides or other reagents was assessed *in vitro* by poison agar assays. Appropriate volumes from stock solutions were added to PDA medium (or WA in the case of treatments containing boscalid or fluopyram) in order to obtain concentrations of 10 μg/mL boscalid, 2 μg/mL fluopyram and tebuconazole, 0.05 μg/mL fluazinam and 0.2 μg/mL fludioxonil individually or in combination with 300 μg/mL ZnO-NPs or 500 μg/mL $ZnSO_4$. The effect of EDTA (100 μg/mL) and SHAM (100 μg/mL) on the sensitivity of isolates to ZnO-NPs or $ZnSO_4$ was also evaluated. Plates inoculated with each *A. alternata* isolate were incubated for 4 days at 25 °C in the dark. Subsequently, mycelial growth was measured in terms of colony diameter and percent inhibition rates were calculated. Synergistic interaction of ZnO-NPs/$ZnSO_4$ with tested antifungal agents was evaluated according to the Abbortt method (Gisi, 1996). Briefly, the expected combined percent inhibition (% CI_{exp}) was calculated as: % $CI_{exp} = I_A + I_B - (I_A \times I_B / 100)$, where I_A and I_B are the percent inhibition of each antifungal agent. Synergy factors (SFs) were determined according to the formula $SF = I_{AB} / (\% CI_{exp})$, where I_{AB} stands for the observed combined percent inhibition of the antifungal agents. SF values close to 1 were considered to indicate additive, greater than 1 synergistic, and less than 0.75 antagonistic interactions.

2.4. Characterization of ZnO-NPs/boscalid mixtures

In an attempt to elucidate the possible mechanism underlying the synergy observed between ZnO-NPs and boscalid against *A. alternata* isolates, suspensions containing 10 μg/mL boscalid, 300 μg/mL ZnO-NPs and their mixture were prepared. All suspensions were subjected to sonication for 30 min to prevent nanoparticle aggregation. Subsequently, zeta potential and hydrodynamic diameter measurements for the ZnO-NPs, boscalid and mixtures were measured in triplicate with a zetasizer (Nano ZS90, Malvern Instruments, Southborough, MA). pH values were also measured for all suspensions using a WTW pH-meter (inoLab® pH 7110).

2.5. Fungitoxicity tests in vivo

The effectiveness of ZnO-NPs alone or in combination with boscalid to control sensitive and fungicide-resistant *A. alternata* isolates *in vivo* was tested using wound-free tomato fruit (*Lycopersicon esculentum* cv mojito) with uniform maturity, shape and size. Four tomato fruits per isolate were treated with ZnO-NPs, boscalid and their combinations and then inoculated with two sensitive (AA236, AA239), one medium (AA203) and one highly (AA171) boscalid-resistant isolates. Control treatment consisted of four tomato fruits spayed with distilled water. Fruits were immersed in a 1% sodium hypochlorite water solution for 10 min in order to be surface-disinfected. Following disinfection, the fruit were rinsed three times with distilled-sterilized water and left to dry before treatment with boscalid or ZnO-NPs. Dry fruits were then sprayed with solutions of 1000 μg/mL ZnO-NPs, 500 and 1000 μg/mL boscalid (1/2, 1 × of the maximum recommended dose) and their combinations. Fruits were left to air-dry for an additional a period of 2 h and then wounded with a lancet creating a 2 × 2 mm [length × width] cross-shaped scar. A 5-mm mycelial plug from the edge of a 4-day old colony from each *A. alternata* isolate was placed on top of each wound. Inoculated fruits were placed inside plastic boxes 24 × 34 × 10 cm [length × width × height] on top of a wet sterilized paper and covered by a lid to ensure moist conditions before incubation at 25 °C in the dark for 4 days. Percent symptom severity was calculated by dividing mean lesion diameter around each wound of treated fruit by the respective lesion diameter of the water-treated control. All experiments were conducted in triplicate.

2.6. DNA extraction and sequence analysis of SDH gene subunits from A. alternata isolates

In an attempt to investigate the resistance mechanism of boscalid-resistant *A. alternata* isolates, 3 subunits (*sdh*B, *sdh*C, *sdh*D) of the gene encoding the succinate dehydrogenase (SDH), target of the SDH-inhibitor fungicides, were amplified and sequenced. Specifically, fungal cultures were grown on fungicide-free PDA at 25 °C for ten days. Subsequently, mycelia were collected by scraping and ground using a mortar and pestle in the presence of liquid nitrogen. Total DNA was isolated using TRI reagent (Sigma) following the manufacturer's instructions. Primer pairs AaSDHB-F (5′ ATACGCGCTTTCACTCGTCT 3′) and AaSDHB-R (5′ GCATGTCCTTG AGCAGTTGA 3′), AaSDHC-F (5′ ATGGCTTCTCAGCGGGTATTTC 3′) and AaSDHC-R (5′ CATCCGAGGAAGGTGTAGTA 3′), AaSDHD-F (5′ GCCTCC GTCATGCGTCCCGG 3′) and AaSDHD-R (5′ CTATGCGTGCCACAACCTC 3′) were used for the amplification of the respective *sdh*B, *sdh*C and *sdh*D gene fragments from each *A. alternata* isolate using gDNA as template. PCR reactions comprised of 0.2 mM from each of the primers, 1.5 mM $MgCl_2$, 0.5 mM dNTPs, and 1.25 units of HotStar Taq DNA polymerase (Qiagen) in 20 mM TrisHCl and 50 mM KCl. The PCR conditions were: 95 °C for 15 min followed by 40 cycles of 94 °C for 30 s, 58 °C for 30 s, and 72 °C for 1 min with a final 10 min extension at 72 °C. QIAquick gel extraction kit (Qiagen) was used to purify PCR products which were subsequently ligated to pGEM-Teasy (Promega) vectors and transformed into *E. coli* competent cells (DH5a Library Efficiency® Competent Cells, Invitrogen). Plasmids containing the *sdh*B, *sdh*C and *sdh*D respective gene fragments were purified using QIAprep spin miniprep kit plasmid (Qiagen)

and then sequenced in both directions. Ten independent clones from each *A. alternata* tested isolate were analyzed. Sequence data analysis was performed using the Lasergene (DNAstar, Madison, USA) software.

3. Statistical analysis

The EC_{50} values for each isolate and fungicide were estimated by regression of the relative inhibition of mycelial growth against the Log_{10} of the compound concentrations. Pearson correlation coefficients were used to evaluate correlation between isolate sensitivities to tested NPs/fungicides. Inhibition rates caused by ZnO-NPs and fungicides were subjected to analysis of variance (ANOVA) while means were separated according to Tukey's HSD test ($\alpha = 0.05$). All statistical analyses were conducted using the SPSS v20 software (SPSS Inc., Chicago, IL, USA).

4. Results

4.1. Sensitivity screening of A. alternata isolates in vitro

Sensitivity of *A. alternata* to ZnO-NPs in terms of EC_{50} values ranged between 250 and 388 μg/mL with a median value of 303 μg/mL. Fungitoxicity tests showed that ZnO-NPs were significantly ($P < 0.01$) more effective against *A. alternata* than its ionic counterpart $ZnSO_4$ or the reference protective fungicide containing $Cu(OH)_2$ *in vitro* (see Table 1). Screening fungicide resistant isolates using discriminatory doses revealed that *A. alternata* isolates exhibited baseline sensitivity to most fungicides tested (see Table 1). This was not the case for boscalid, where all but 2 isolates tested exhibited reduced sensitivity to the SDHI boscalid (see Tables 1, 2), probably due to the extensive use of this class of fungicides against the pathogen during the last years. Resistance factors (Rfs) for boscalid and fluopyram, of SHHI-resistant isolates were calculated based on EC_{50} values determined by additional fungitoxicity tests (see Table 2). Analysis revealed one *A. alternata* isolate (AA171) highly resistant (BOSC-HR) to SDHIs boscalid and fluopyram (Rf: >96 and 145 respectively), seven isolates with medium resistance (BOSC-MR) to boscalid but not to fluopyram (Rf: 28.44–36.76) and two isolates (AA236, AA239) sensitive to both boscalid (BOSC-S) and fluopyram (see Table 2).

4.2. Identification of target-site resistance mutations

The existence of resistance mutations in the gene encoding the target site of SDHI fungicides in the BOSC-MR/HR isolates was validated by sequencing *sdh*B, *sdh*C, and *sdh*D gene fragments isolated from sensitive and resistant isolates.

Sequencing analysis and comparison of the deduced amino-acid sequence between BOSC-M/HR and BOSC-S isolates revealed an alanine (A: GCC) substitution by threonine (T: ACC) at position 47 of the *sdh*D protein leading to the A47T resistance mutation in all boscalid resistant isolates. An additional resistance mutation was found in the highly boscalid and fluopyram resistant AA171 isolate resulting from the replacement of histidine (H: CAC) with arginine (CGC) at position 134 (H134R) of the *sdh*C protein (see Table 2). The H134R amino acid substitution is a well-documented SDHI resistance mutation, known to confer high resistance levels in *A. alternata* and *A. solani* (Sang and Lee, 2020). These results indicated that target-site modification reducing the affinity between boscalid and their succinate dehydrogenase (SDH) target was the mechanism responsible for the observed BOSC-MR and BOSC-HR resistant phenotypes.

Table 2
Sensitivity profiles of representative *A. alternata* isolates to SDHI fungicides boscalid and fluopyram and respective resistance mutations in the target site gene subunits (*sdh*B, *sdh*C, *sdh*D).

Isolate	Fungicides				Succinate dehydrogenase gene subunits amino acid substitutions		
	Boscalid		Fluopyram		*sdh*B	*sdh*C	*sdh*D
	EC_{50}[a] (mean ± SD[b])	Rf[c]	EC_{50} (mean ± SD)	Rf			
AA236	1.55 ± 0.25	1.00	0.04 ± 0.01	1.33	–	–	–
AA239	1.65 ± 0.30	1.06	0.03 ± 0.00	1.00	–	–	–
AA201	56.37 ± 3.36	36.37	0.05 ± 0.02	2.50	–	–	A47T
AA234	44.09 ± 2.51	28.44	0.10 ± 0.05	3.33	–	–	A47T
AA191	45.62 ± 3.70	29.32	0.15 ± 0.10	5.00	–	–	A47T
AA203	52.60 ± 5.18	33.93	0.08 ± 0.02	2.66	–	–	A47T
AA202	48.29 ± 4.07	31.15	0.11 ± 0.04	3.67	–	–	A47T
AA204	54.22 ± 4.05	34,98	0.09 ± 0.02	3.00	–	–	A47T
AA235	56.98 ± 1.88	36.76	0.12 ± 0.04	4.00	–	–	A47T
AA171	>150	>96.77	4.35 ± 0.05	145.0	–	H134R	A47T

[a] Effective concentration causing 50% reduction in mycelial growth rate after a 4-day incubation period at 25 °C (n = 3).
[b] Standard deviation of the means (n = 3).
[c] Resistance factor (EC_{50} of each isolate/mean EC_{50} of the most sensitive isolate).

4.3. Synergy between ZnO-NPs and fungicides

4.3.1. In vitro bioassays

ZnO-NPs were tested *in vitro* against sensitive and boscalid-resistant *A. alternata* isolates in combination with boscalid, fluopyram, fludioxonil, tebuconazole, SHAM, EDTA, and fluazinam. Similar tests were carried out to evaluate potential synergism between $ZnSO_4$ and boscalid, fluopyram, EDTA, and SHAM. Synergy factors (SF) were calculated for ZnO-NPs/$ZnSO_4$ and combinations and the respective values are shown in Table 4. ZnO-NPs significantly enhanced the fungitoxic effect of boscalid against both BOSC-S and BOSC-M/HR *A. alternata* isolates, resulting in almost complete inhibition of mycelial growth in most cases (see Figs. 1a, 2). SF values between ZnO-NPs and boscalid ranged between 1.08 and 2.57 (see Table 3). Contrary to the profound synergistic profile exhibited by ZnO-

Table 1
Sensitivity of *Monilinia fructicola* isolates to Ag-NPs and selected fungicides.

Isolate	Percent inhibition[a] (mean ± SD[b])								
	ZnO-NPs (500)[c]	$ZnSO_4$ (500)	$Cu(OH)_2$ (500)	Mancozeb (100)	Boscalid (10)	Fluopyram (2)	Tebuconazole (2)	Fluazinam (0.05)	Fludioxonil (0.2)
AA201	64.41 ± 0.35	53.33 ± 0.11	51.32 ± 1.05	25.35 ± 0.71	42.55 ± 0.71	100	64.79 ± 1.41	40.84 ± 0.29	93.65 ± 0.24
AA234	53.65 ± 1.51	35.56 ± 0.18	38.50 ± 3.02	24.24 ± 2.83	55.58 ± 1.41	100	53.03 ± 0.74	30.11 ± 1.32	61.82 ± 2.57
AA191	65.59 ± 0.96	66.67 ± 1.01	40.89 ± 2.10	35.29 ± 2.83	53.33 ± 1.41	100	70.59 ± 0.28	26.31 ± 1.04	93.22 ± 2.30
AA203	64.18 ± 2.15	71.67 ± 0.50	41.12 ± 3.05	22.86 ± 0.05	46.67 ± 0.02	100	65.71 ± 0.83	32.69 ± 0.17	64.71 ± 2.28
AA202	77.86 ± 1.10	30.23 ± 1.00	39.14 ± 2.85	32.26 ± 0.12	57.78 ± 0.10	100	66.13 ± 0.04	59.78 ± 0.67	72.31 ± 0.75
AA236	63.70 ± 3.10	49.23 ± 0.71	28.96 ± 3.54	28.57 ± 0.71	95.1 ± 0.09	100	50.79 ± 0.00	25.05 ± 1.09	53.85 ± 5.44
AA204	67.41 ± 2.55	60.32 ± 0.71	37.10 ± 0.10	32.43 ± 0.06	48.94 ± 0.05	100	66.22 ± 1.25	19.51 ± 0.25	73.53 ± 4.16
AA239	66.22 ± 1.68	38.46 ± 1.41	50.12 ± 1.65	34.29 ± 4.24	93.81 ± 0.16	100	60.05 ± 0.92	28.03 ± 2.10	47.54 ± 3.45
AA171	65.72 ± 1.54	73.08 ± 0.17	54.19 ± 6.19	13.85 ± 2.83	1.00 ± 0.03	58.52 ± 3.54	69.23 ± 0.06	23.68 ± 2.14	100. ± 0.00
AA235	62.08 ± 3.13	35.82 ± 0.68	12.32 ± 1.53	28.99 ± 0.71	41.88 ± 0.71	100	55.07 ± 0.77	28.04 ± 1.22	65.52 ± 5.22

[a] Calculated as percent inhibition of mycelial growth compared to the untreated control after a 4-day incubation period at 25 °C (n = 3).
[b] Standard deviation of the means (n = 3).
[c] Numbers in parenthesis indicate fungicide concentrations in μg/mL of active ingredient.

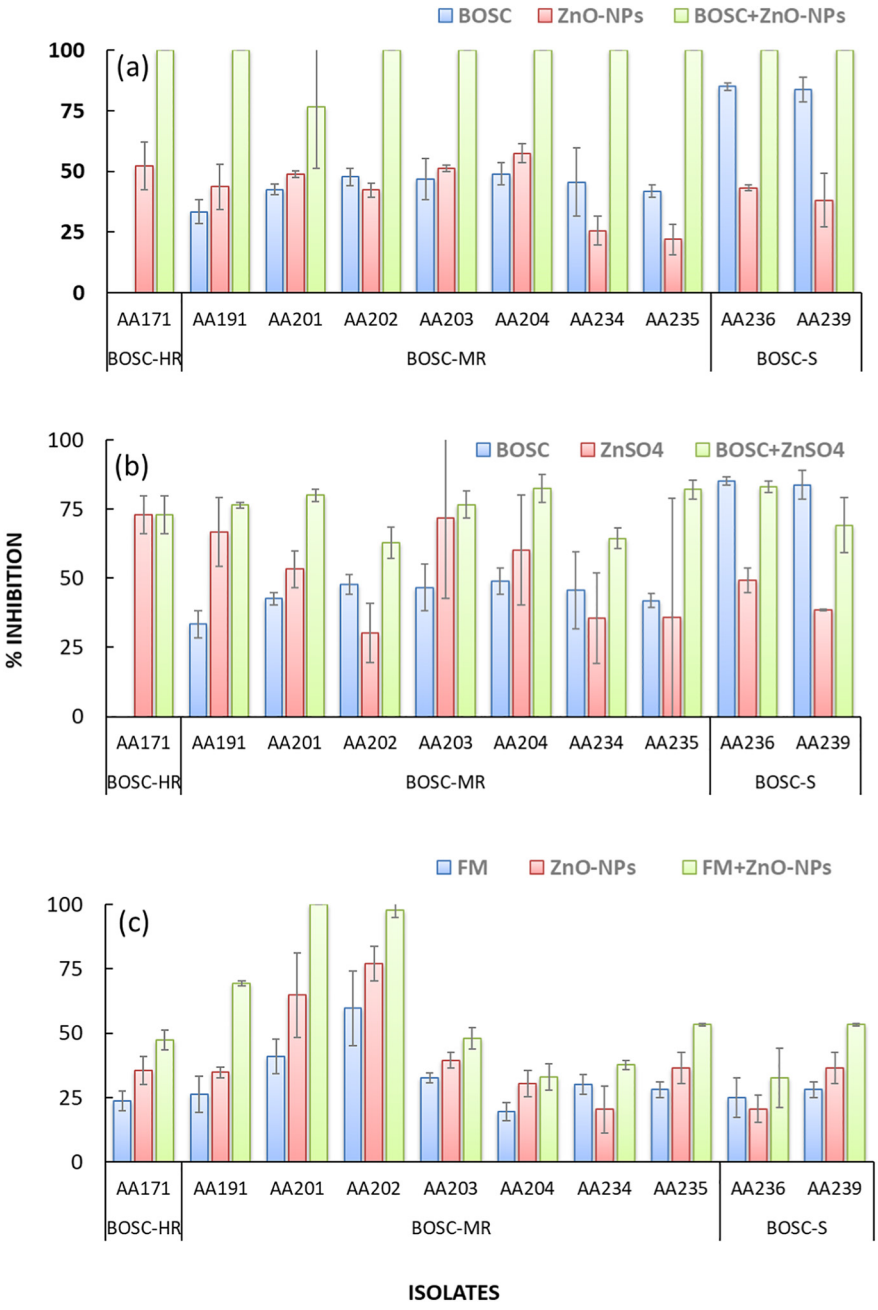

Fig. 1. Sensitivity of fungicide-sensitive/resistant *A. alternata* isolates to boscalid (10 μg/mL) in comparison with: (a) ZnO-NPs (300 μg/mL), (b) $ZnSO_4$ (500 μg/mL), and fluazinam (0.2 μg/mL) with (c) ZnO-NPs (300 μg/mL) and their combinations. BOSC-S/MR/HR: boscalid-sensitive/moderately or highly resistant isolates (BOSC: boscalid, FM: fluazinam). Error bars represent the standard deviation of means. Between treatments, bars marked by the same letter do not differ significantly according to Tukey's HSD test ($\alpha = 0.05$).

NPs, the combined use of its ionic counterpart $ZnSO_4$ with boscalid resulted in a mostly additive effect with SF values ranging between 0.85 and 1.06 (see Table 3, Fig. 1b), probably indicating an additional role of nanoparticle properties to the observed synergism between ZnO-NPs and boscalid other than zinc ion release. An additive or synergistic effect (SF: 0.91–1.34) was observed between ZnO-NPs and fluazinam (see Table 3). In most cases, the addition of fluazinam enhanced toxicity of ZnO-NPs while, in some BOSC-MR cases, it led to complete inhibition of mycelial growth (Fig. 1c). A slight additive effect was observed in the cases of ZnO-NPs/fludioxonil (SF: 0.80–1.17) and ZnO-NPs/tebuconazole (SF: 0.80–0.89) combinations (see Table 3).

The possible role of zinc ions release on the fungitoxic mode of action of ZnO-NPs was investigated by combining them with the strong chelating agent EDTA in a synergism bioassay *in vitro*. Addition of 100 μg/mL EDTA in growth medium containing 300 μg/mL ZnO-NPs resulted in the alleviation of the fungitoxic effects of the zinc oxide nanoparticles against *A. alternata* indicating that zinc ion release contributes, at least partly, on the nanoparticle inhibitory action. This was evident on the synergy factor values between ZnO-NPs and EDTA that ranged between 0.16 and 0.60 suggesting a strong antagonistic effect (see Table 3). A similar antagonistic effect was observed between $ZnSO_4$ and EDTA in most isolate cases.

In a similar context, aiming to investigate the involvement of the ROS generation on the fungitoxic mode of action of ZnO-NPs, the alternative oxidase (AOX) specific inhibitor SHAM was employed. Inhibiting the AOX pathway with SHAM resulted in an enhanced fungitoxic effect of both ZnO-NPs and its ionic counterpart $ZnSO_4$. Synergy factor values recorded were close to 1 in both cases indicating an additive effect (see Table 3).

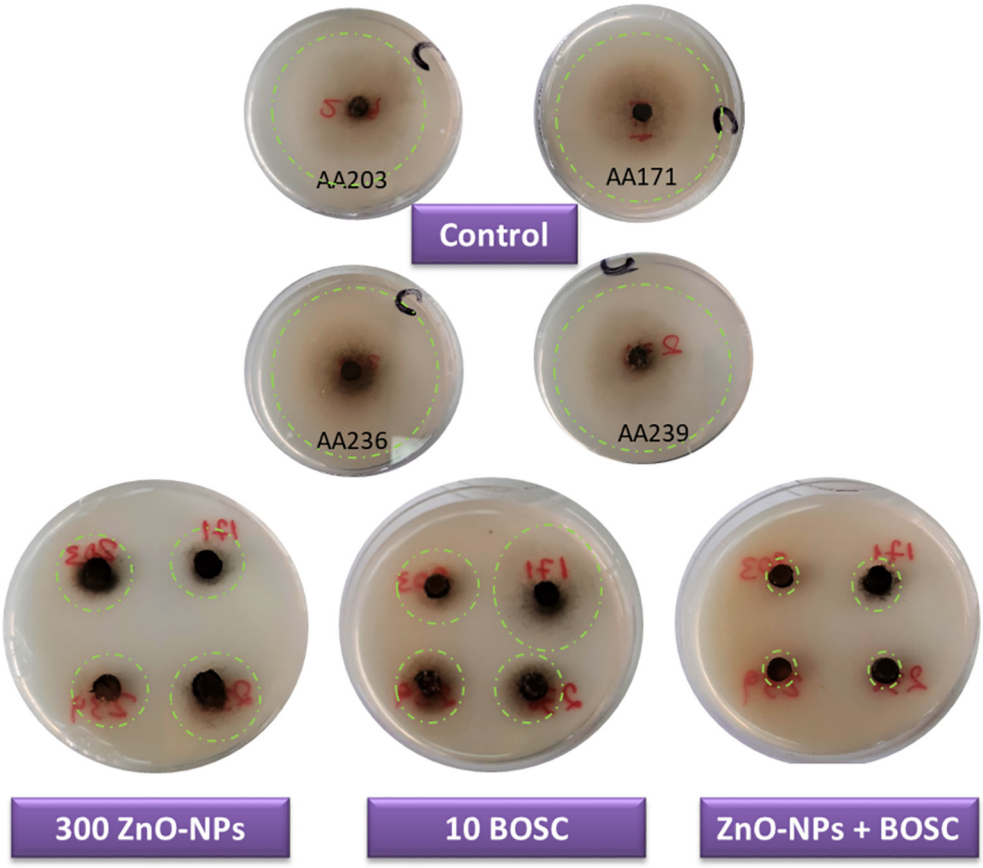

Fig. 2. Fungitoxic activity of ZnO-NPs, boscalid (BOSC) and their combination in sensitive (AA236, AA239), moderately (AA203) and highly (AA171) boscalid-resistant *Alternaria alternata* isolates. Green dashed circles indicate colony margins.

4.3.2. In vivo bioassays

The synergistic activity between ZnO-NPs and boscalid against both sensitive and boscalid-resistant *A. alternata* isolates observed *in vitro*, was tested on tomato fruit inoculated with representative isolates from each phenotypic category. The addition of boscalid significantly enhanced percent disease suppression caused by ZnO-NPs (see Fig. 3). Specifically, percent inhibition of lesion development in ZnO-NPs/boscalid combinations ranged between 34.21 and 82.32%, while the respective values for ZnO-NPs alone ranged between 0 and 32.25% (see Table 4). Synergy factors (SF: 1.18 to 1.57) between ZnO-NPs and boscalid clearly indicated a strong synergistic effect between the two antifungals confirming the findings of the *in vitro* experiments.

4.3.3. Characterization of ZnO-NPs, boscalid and mixture

Size, charge and pH values of 10 μg/mL boscalid, 300 μg/mL ZnO-NPs and their mixture are shown in Table 5. Mean hydrodynamic diameter of ZnO-NPs were measured to be 237.3 nm, while boscalid had a respective value of 360.2 nm. Interestingly, their mixture resulted in a homogenous

Table 3
In vitro synergistic activity of ZnO-NPs or $ZnSO_4$ with selected fungicides against boscalid sensitive and resistant *Alternaria alternata* isolates (BOSC: boscalid, FLUO: fluopyram, FM: fluazinam, TEB: tebuconazole, FLUD: fludioxonil).

Isolate	Resistance phenotype	SF[a]										
		ZnO-NPs (300)							$ZnSO_4$ (500)			
		BOSC (75)[c]	FLUO (2)	FM (0.05)	EDTA (100)	SHAM (100)	TEB (2)	FLUD (0.2)	BOSC (75)	FLUO (2)	EDTA (100)	SHAM (100)
AA236	BOSC-S[b]	1.45	1.04	0.91	0.38	1.35	0.86	0.87	1.03	0.91	0.52	0.93
AA239	BOSC-S	1.89	0.91	0.98	0.44	0.98	0.80	0.80	0.85	0.81	1.80	1.05
AA201	BOSC-MR	1.08	0.76	1.26	0.51	0.99	0.88	0.98	1.04	1.01	0.42	1.09
AA234	BOSC-MR	2.24	0.69	0.95	0.52	0.84	0.89	0.81	0.94	0.96	2.25	0.84
AA191	BOSC-MR	1.60	1.60	1.34	0.16	0.94	0.80	0.98	0.86	0.91	1.02	0.82
AA203	BOSC-MR	1.35	2.11	0.91	0.52	0.96	0.88	0.90	0.87	1.05	0.20	1.09
AA202	BOSC-MR	1.15	1.21	1.08	0.35	1.75	0.89	1.17	1.06	0.97	0.49	1.02
AA204	BOSC-MR	1.28	0.99	0.95	0.60	1.17	0.81	0.90	1.00	0.89	0.38	1.28
AA235	BOSC-MR	2.57	0.97	0.98	0.51	0.86	0.88	1.02	1.03	0.86	0.55	0.89
AA171	BOSC-HR	1.89	1.46	0.93	0.61	0.99	0.83	1.02	0.92	2.23	0.54	1.01

[a] Synergy factor.
[b] BOSC-S: boscalid sensitive, BOSC-MR/HR: boscalid medium/highly resistant isolate.
[c] Numbers in parenthesis indicate antifungal agent concentrations in μg/mL of active ingredient.

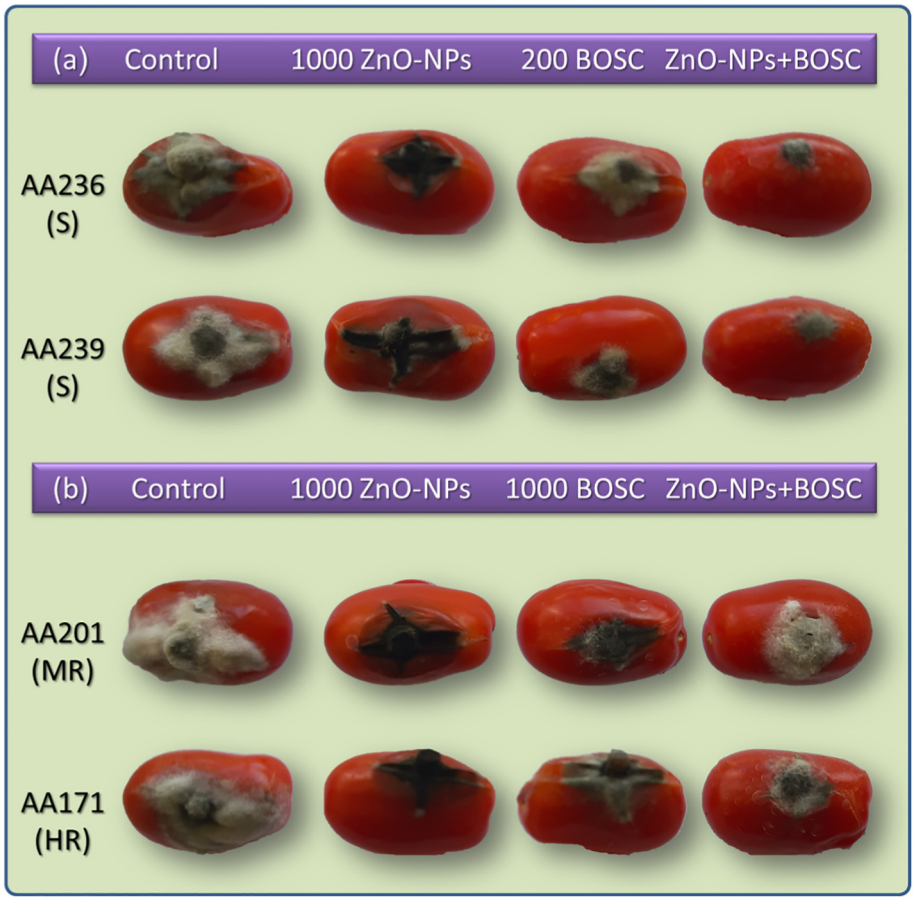

Fig. 3. Synergistic activity of ZnO-NPs (1000 μg/mL) in combination with boscalid (200/1000 μg/mL) against representative (a) sensitive and (b) medium (AA201) or highly (AA171) boscalid-resistant *Alternaria alternata* isolates (BOSC: boscalid).

suspension of particles with a mean size of 169.6 nm and a similar to boscalid distribution (see Table 5, Fig. 4). Furthermore, the addition of the negatively charged boscalid (−42.4 mV) to positively charged ZnO-NPs (25.9 mV) resulted in an also negatively charged (−35.6 mV) suspension of ZnO-NPs-boscalid conjugates. This negative charge probably acted as a dispersive factor resulting to a homogenous suspension with lower hydrodynamic particle sizes. This reduction in nanoparticle size could be a reason for the enhanced fungitoxic effect of the ZnO-NPs + boscalid mixture compared to ZnO-NPs alone.

Table 5
Zeta potential, diameter size and pH values of ZnO-NPs (300 mg/mL), boscalid (10 mg/mL) and mixture.

	pH	Zeta potential (mV) (mean ± SD[a])	Size (d·nm) (mean ± SD)
ZnO-NPs	7.0	25.9 ± 0.2	237.3 ± 2.7
boscalid	5.7	−42.4 ± 5.5	360.2 ± 4.1
ZnO-NPs + boscalid	6.7	−35.6 ± 1.5	169.6 ± 1.0

[a] Standard deviation of the means (n = 3).

Table 4
Synergistic activity of ZnO-NPs co-applied with boscalid on tomato fruit against *Alternaria alternata* isolates sensitive and resistant to boscalid (BOSC) fungicide.

Isolate	Phenotype	Percent inhibition[a] (mean ± SD[b])				
		ZnO-NPs (1000)[d]	BOSC (500/1000[e])	ZnO-NPs + BOSC	Expected inhibition (%)	SF[f]
AA236	BOSC-S[c]	14.24 ± 3.19	44.42 ± 2.35	82.32 ± 0.12	52.33	1.57
AA239	BOSC-S	2.05 ± 1.52	50.35 ± 3.08	74.56 ± 1.05	51.37	1.45
AA191	BOSC-MR	32.50 ± 0.13	30.25 ± 0.75	80.34 ± 3.42	52.92	1.52
AA201	BOSC-MR	16.98 ± 2.45	19.06 ± 1.17	43.40 ± 0.88	32.80	1.32
AA203	BOSC-MR	0.00	28.95 ± 2.90	34.21 ± 1.45	28.95	1.18
AA171	BOSC-HR	22.81 ± 2.06	10.05 ± 0.05	52.63 ± 3.19	30.57	1.72

[a] Calculated as percent inhibition of lesion development on apple fruit sprayed with ZnO-NPs/fungicides and their combinations compared to the untreated control after 4-day incubation period at 25 °C (n = 3).
[b] Standard deviation of the means (n = 3).
[c] BOSC-S: boscalid sensitive, BOSC-MR/HR: boscalid medium/highly resistant isolate.
[d] Numbers in parenthesis indicate fungicide concentrations in μg/mL of active ingredient.
[e] Boscalid concentrations applied on tomato fruit were 500 μg/mL for the BOSC-S and 1000 μg/mL for the BOSC-MR/HR isolates.
[f] Synergy Factor calculated as observed inhibition caused by the ZnO-NPs + BOSC mixture over the expected inhibition by the individual treatments.

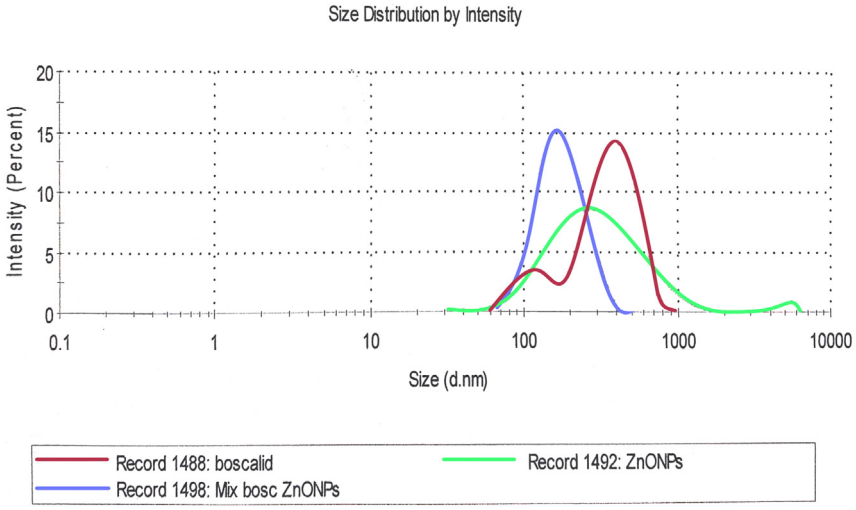

Fig. 4. Mean size distribution of boscalid (10 μg/mL), ZnO-NPs (300 μg/mL) particles and their mixture measured by dynamic light scattering.

4.4. Sensitivity correlations between ZnO-NPs, $ZnSO_4$, antifungal agents and combinations

In order to investigate the possible mode of action of ZnO-NPs or its contribution in the observed synergistic relationship with fungicides or reagents tested, correlations were calculated using Pearson correlation coefficients (see Table 6, Fig. 5). The significant correlation (r = 0.73, P = 0.05) found between ZnO-NP and $ZnSO_4$ indicated a similar mode of action between the counterparts suggesting that zinc ion release plays an important role in the observed antifungal action of ZnO-NPs (See Fig. 5a). Both ZnO-NPs and fluazinam seem to contribute on the observed additive fungitoxic effect of their combination as indicated by the positive correlation of each of both antifungals with ZnO-NPs + fluazinam in terms of sensitivity (see Fig. 5d). On the contrary, no statistically significant correlation was observed between ZnO-NPs, boscalid and their combination (see Table 6). A positive correlation (r = 0.67, P = 0.05) was found between boscalid and fluazinam, while a negative one between boscalid and SHAM (see Table 6, Fig. 5c). Sensitivity of *A. alternata* to ZnO-NPs was positively correlated with their respective sensitivity to EDTA as shown in Fig. 5b.

5. Discussion

The potential of ZnO-NPs to control sensitive and boscalid resistant *A. alternata* isolates collected from Greek tomato-growing greenhouses was evaluated by bioassays conducted both *in vitro* and *in vivo*. Sensitivity screening of *A. alternata* isolates revealed 3 boscalid-sensitivity phenotypes: sensitive (S), moderately (MR), and Highly (HR) boscalid resistant. Sequencing analysis of the succinate dehydrogenase (SDH) gene, encoding the target enzyme of the SHDI boscalid revealed one resistance mutation (A47T) in the *sdh*D subunit of the gene, present in all resistant phenotypes. An additional mutation (H134R) in the *sdh*C subunit was found in the case of the AA171 HR isolate. The H134R mutation has been implicated with high-level SDHI-resistance in various plant pathogens while the A47T has only been reported in *A. alternata* (Sang and Lee, 2020; Sierotzki and Scalliet, 2013; Malandrakis et al., 2018). These results confirmed that target site modification was the main resistance mechanism of MR and HR isolates. Subsequently, characterized sensitive and boscalid resistant isolates were utilized to evaluate the effectiveness of ZnO-NPs as antifungal agents and their potential as fungicide-partners in the combat against drug-resistance.

Table 6
Correlation between sensitivity of *A. alternata* isolates to ZnO-NPs, $ZnSO_4$, boscalid (BOSC), fluazinam (FM) and their combinations.

	ZnO-NPs	$ZnSO_4$	BOSC	FM	ZnO-NPs + BOSC	ZnO-NPs + FM
ZnO-NPs	1.0[a]	0.73*	0.23	0.88**	0.32	0.92**
$ZnSO_4$	–	1.0	−0.27	−0.46	−0.04	−0.20
BOSC	–	–	1.0	0.672*	−0.10	0.43
FM	–	–	–	1.0	−0.28	0.81**
ZnO-NPs + BOSC	–	–	–	–	1.0	−0.61
ZnO-NPs + FM	–	–	–	–	–	1.0

[a] Pearson correlation coefficient values.
* Corresponds to a significance lever of P = 0.05.
** Corresponds to a significance lever of P = 0.01.

Research on metal nanoparticles used as antibiotic alternatives/partners is gaining ground following their successful use against life-threatening clinical drug or multi drug-resistant (MDR) pathogens (Jampilek, 2016; Punjabi et al., 2018). The majority of these studies are about bacterial infections due to their importance in human health, while limited are the reports available on the respective interaction of metal nanoparticles with fungicides controlling sensitive or, even less, with drug-resistant fungal strains (Malandrakis et al., 2021b). Polyvinylpyrrolidone (PVP)-coated Ag-NPs were shown to be effective against the drug-resistant strains of the human fungal pathogen *Candida albicans* alone or in combination with sterol biosynthesis inhibiting fungicides (Sun et al., 2016). In the case of plant pathogenic fungi, an enhanced toxicity of Ag-NPs and ZnO-NPs combined with fungicides carbendazim, mancozeb and thiram, was reported against *B. cinerea*, *A. alternata*, *Fusarium oxysporum*, *Aspergillus niger* and, *Penicillium expansum* (Jamdagni et al., 2018). Synergy as well as photo-degradation properties of ZnO-NPs when applied with the fungicide thiram were also reported *Phytophthora capsici* (Xue et al., 2014). Recent studies have revealed successful antifungal potential of silver and copper containing NPs against sensitive or benzimidazole-resistant strains of *B. cinerea* and *M. fructicola*, which was enhanced when combined with fungicides thiophanate methyl or fluazinam (Malandrakis et al., 2020a, 2020b, 2021b).

ZnO nanoparticles tested in this study, were effective against both sensitive and boscalid resistant *A. alternata* isolates and even more effective in comparison with their ionic counterpart $ZnSO_4$ or the reference protective fungicide containing $Cu(OH)_2$. When used in combination with boscalid, a profound enhancement of the fungitoxic effect of ZnO-NPs against both sensitive and boscalid-resistant *A. alternata* isolates was observed *in vitro*. No synergy was observed between boscalid and $ZnSO_4$ indicating that nanoparticle properties probably account for enhanced toxicity of boscalid + ZnO-NPs treatment. This synergistic effect was also demonstrated *in vivo*, where the treatment of tomato fruits with the boscalid + ZnO-NPs combination significantly increased the suppression of disease

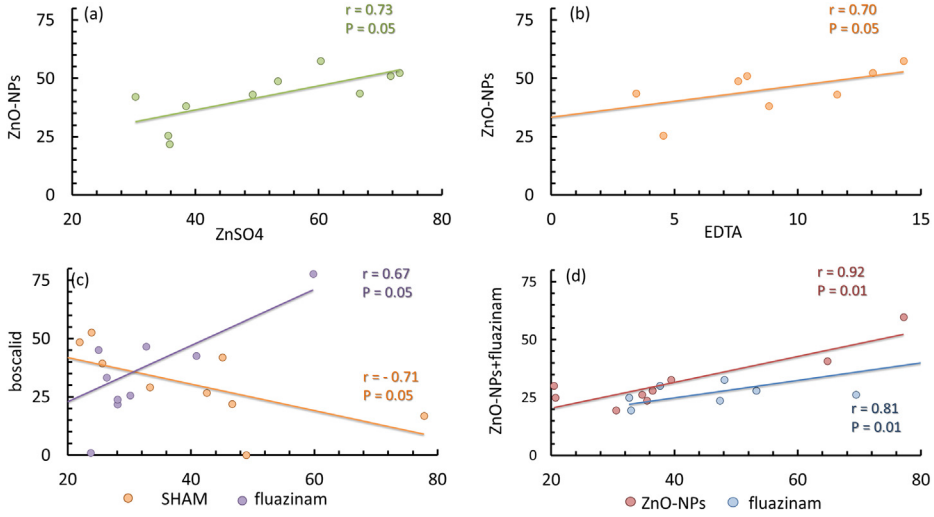

Fig. 5. Correlation between sensitivities of *A. alternata* isolates to ZnO-NPs (300 μg/mL) and (a) $ZnSO_4$ (500 μg/mL), (b) EDTA (100 μg/mL), (c) boscalid (10 μg/mL) and SHAM (100 μg/mL) or fluazinam (0.05 μg/mL), and (d) fluazinam (0.05 μg/mL) and ZnO-NPs alone or in combination with fluazinam. Here, r is the Pearson correlation coefficient, and P the significance level.

symptoms compared to the individual treatments. The similar ZnO-NPs/boscalid synergy factor values between isolates belonging to different boscalid sensitivity phenotypes suggest that the enhanced toxicity observed could more likely be attributed to ZnO-NPs rather than boscalid. This is in agreement with a previous study where synergy observed between Ag-NPs and thiophanate methyl (TM) against *M. fructicola* was also attributed to an enhanced NP toxicity (Malandrakis et al., 2020b). On the contrary, when Cu-NPs and TM mixtures were utilized against *B. cinerea* or *M. fructicola*, synergy observed most likely resulted from a higher fungicide bioavailability (Malandrakis et al., 2020a, 2021b). In the present study, mixture of ZnO-NPs with boscalid resulted in a significantly reduced NP size as assessed by dynamic light scattering (DLS) using a Zetasizer. This reduction in nanoparticle size could be responsible for the increased toxicity exerted by the mixture compared with the ZnO-NPs alone. Several studies have indicated that smaller size of NPs leads to a more favorable surface area-to-volume ratio that promotes their antifungal activity although size is not the only major factor affecting NP toxicity (Kalia et al., 2021; Cruz-Luna et al., 2021). Another plausible explanation for the enhanced ZnO-NPs toxicity when combined with boscalid could involve a drug-facilitated mechanism that modulates delivery of the NPs inside the fungal cell. A recent study by Kalampokis et al. (2018), utilizing *A. nidulans* genetically inactivated mutants, has demonstrated that boscalid uptake is mediated by several nucleobase membrane transporters. It is possible that boscalid particles decorated with ZnO-NPs are "recognized" by those nucleobase transporters and are transferred inside the fungal cell where they can exert an additional toxic action by generating reactive oxygen species (ROS) or interacting with proteins and enzymes crucial for fungal metabolism. Typically, direct contact of the positive charged ZnO-NPs with the fungal membrane is mediated by electrostatic attraction with the negative charged cell surface (Ruddaraju et al., 2020). On the contrary, ZnO-NPs + boscalid conjugates were negatively charged and thus are expected to be repelled by the also negatively charged fungal membrane. Internalization of the NP-drug conjugate by the above-mentioned transporters could bypass this obstacle and allow ZnO-NPs to exert their fungitoxic action internally and more effectively.

The fungitoxic action of metal NPs has been attributed to mechanisms that lead to disruption of cell walls or membrane integrity, generation of ROS, protein inactivation, disruption of the electron transport chain, damage to DNA and, eventually, cell death (Rudramurthy et al., 2016; Ruddaraju et al., 2020; Nisar et al., 2019; Cruz-Luna et al., 2021; Márquez et al., 2018). Metallic counterparts of NPs in their ionic form share the same or similar mechanisms of toxic action against pathogens giving rise to the question whether toxicity is caused by the metal ions escaping nanoparticle surfaces or by the unique NP properties (Sun et al., 2018; Hoseinzadeh et al., 2017; Król et al., 2017; Robinson et al., 2021; Slavin et al., 2017). In an attempt to resolve this debate, several approaches have been utilized involving biochemical, genomic, transcriptomic, and metabolomic methods (Márquez et al., 2018; Cruz-Luna et al., 2021; Kumari et al., 2019; Sardella et al., 2017). Zinc ion accumulation facilitated by zinc transporters was reported to be responsible for the fungitoxic action of ZnO-NPs in *Sclerotinia homeocarpa* (Li et al., 2017). High throughput Gene Deletion Analysis (GDA) of *C. serevisiae* mutants highly sensitive to ZnO-NPs revealed that transmembrane transport and cellular ion homeostasis play a pivotal role in ZnO-NPs antifungal activity (Márquez et al., 2018).

In the present study, a strong chelating agent (EDTA) was added in ZnO-NPs containing treatments in order to arrest Zn^{+2} cations dissolving from NPs. This resulted in a significant alleviation of the toxic effect of ZnO-NPs against *A. alternata* suggesting that ion release is mainly responsible for the fungitoxic action of ZnO-NPs. This was also confirmed by the positive correlation found between $ZnSO_4$ and ZnO-NPs sensitivities in the respective *A. alternata* fungitoxicity bioassays. This is in agreement with a previous study by Sardella et al. (2017) where, EDTA caused inactivation of ZnO-NPs toxic activity against the postharvest plant pathogen *P. expansum*. The same antagonistic effect between EDTA and Cu-NPs was observed in the case of *M. fructicola* but not when Ag-NPs were used instead of copper NPs indicating that ion release role in toxicity could vary between different metal NPs (Malandrakis et al., 2020b, 2021b). Another possible mechanism of fungitoxic action of ZnO-NPs against *A. alternata* involving ROS was evaluated using SHAM, a specific inhibitor which blocks the alternative oxidase antioxidant action. When the ROS scavenging function by AOX was inhibited with SHAM, the fungitoxic effect of ZnO-NPs was enhanced indicating that ROS generation could contribute to augmenting the action of NPs. Some ROS such as H_2O_2, produced by the interaction of NPs with the cell membrane proteins, can penetrate cell membrane and cause damage to proteins, enzymes or DNA (Cruz-Luna et al., 2021; Slavin et al., 2017; Arciniegas-Grijalba et al., 2019). NPs properties that affect their size and shape such as the presence of edges or defects could enhance their ability to generate ROS (Slavin et al., 2017). Nevertheless, synergy factor values between SHAM and ZnO-NPs or its ionic counterpart $ZnSO_4$ in *A. alternata* were similar indicating no quantitative differences between Zn-ion and NPs mediated ROS generation mechanism. However, given that ZnO-NPs were more toxic compared to their ionic counterpart, an additional potential mechanism must be responsible for the observed fungitoxic action of the NPs to *A. alternata*.

Fungi utilize specific zinc transporters that are responsible for Zn^{+2} ion influx, cytosol and vacuole transport and ion efflux as a part of their cellular

ion homeostasis mechanism (Li et al., 2017; Robinson et al., 2021). Zinc toxicity results from the excessive number of ions present outside or inside the fungal cell and the inability of the ion homeostatic mechanism to cope with the accumulated ion load. Cellular defense mechanisms include extracellular inhibition of ion uptake/internalization and intracellular compartmentalization, binding with biomolecules or active efflux of metal ions (Priyadarshini et al., 2021). Differences in the level of toxicity of NPs compared to their ionic counterparts could result from the way they are distributed around the fungal cell. Metal ions are uniformly distributed around fungal cells without specific localization in contrast with the larger NPs, which are unevenly distributed around cells creating focal sources of continuously released ions. This large NP-generated ion concentration induces ion penetration and impairs ion homeostatic mechanisms that cannot cope with the ion release rates produced, thus causing a more profound toxic effect than individual metal ions. This could explain the superior fungitoxic effect of ZnO-NPs against *A. alternata* compared to $ZnSO_4$. The synergistic/additive effect observed between fluazinam (an ATP-synthetase inhibitor) and ZnO-NPs could also be an indication that an efflux mechanism regulating zinc ion homeostasis is involved in the toxicity of ZnO-NPs (Kalamarakis et al., 2000; Leroux and Walker, 2013).

In summary, ZnO-NPs were effective against *A. alternata* sensitive and resistant to boscalid phenotypes and exhibited an enhanced antifungal activity when applied in combination with boscalid or fluazinam. Zinc ion release is probably the main mechanism of ZnO-NPs mode of fungitoxic action, which is superior to its ionic counterpart $ZnSO_4$ probably due to NPs ROS production or the inability of the fungal ion homeostasis mechanism to cope with the excessive ion dissolution rate of the NPs. Synergy between boscalid and ZnO-NPs probably results from a potential capping effect that reduces ZnO nanoparticle size. These results highlight the promising potential of ZnO-NPs to be used as antifungal agents for both combating fungicide-resistance and reducing environmental impact of synthetic fungicides, although further studies concerning their safe use, effect on plant health and fruit quality are needed before their introduction as alternative fungicides.

Ethical approval

This article does not contain any studies with human participants or animals performed by any of the authors.

CRediT authorship contribution statement

Anastasios A. Malandrakis: Conceptualization, Investigation, Methodology, Writing. **Nektarios Kavroulakis**: Investigation, Visualization, Reviewing. **Constantinos V. Chrysikopoulos**: Supervision, Visualization, Reviewing and Editing.

Declaration of competing interest

The authors declare that they have no known competing financial interests or personal relationships that could have appeared to influence the work reported in this paper.

References

Arciniegas-Grijalba, P.A., Patiño-Portela, M.C., Mosquera-Sánchez, L.P., Guerra Sierra, B.E., Muñoz-Florez, J.E., Erazo-Castillo, L.A., Rodríguez-Páez, J.E., 2019. ZnO-based nanofungicides: synthesis, characterization and their effect on the coffee fungi mycena citricolor and colletotrichum sp. Mater. Sci. Eng. C 98, 808–825.

Ashajyothi, C., Prabhurajeshwar, C., Handral, H.K., Kelmani, C.R., 2016. Investigation of antifungal and anti-mycelium activities using biogenic nanoparticles: an eco-friendly approach. Environ. Nanotechnol. Monit. Manag. 5, 81–87.

Avenot, H., Morgan, D.P., Michailides, T.J., 2008. Resistance to pyraclostrobin, boscalid and multiple resistance to pristine ® (pyraclostrobin + boscalid) fungicide in Alternaria alternata causing alternaria late blight of pistachios in California. Plant Pathol. 57, 135–140.

Avenot, H.F., Michailides, T.J., 2015. Detection of isolates of Alternaria alternata with multiple-resistance to fludioxonil, cyprodinil, boscalid and pyraclostrobin in California pistachio orchards. Crop Prot. 78, 214–221.

Bartlett, D.W., Clough, J.M., Godwin, J.R., Hall, A.A., Hamer, M., Parr-Dobrzanski, B., 2002. The strobilurin fungicides. Pest Manag. Sci. 58, 649–662.

Cruz-Luna, A.R., Cruz-Martínez, H., Vásquez-López, A., Medina, D.I., 2021. Metal nanoparticles as novel antifungal agents for sustainable agriculture: current advances and future directions. J. Fungi 7 (12), 1033. https://doi.org/10.3390/jof7121033.

Davis, R., Miyao, E., Mullen, R., Valencia, J., May, D., Gwynne, B., 1997. Benefits of applications of chlorothalonil for the control of black mold of tomato. Plant Dis. 81, 601–603.

Fan, Z., Yang, J.-H., Fan, F., Luo, C.-X., Schnabel, G., 2015. Fitness and competitive ability of Alternaria alternata field isolates with resistance to SDHI, QoI, and MBC fungicides. Plant Dis. 99, 1744–1750.

Gabrielyan, L., Hakobyan, L., Hovhannisyan, A., Trchounian, A., 2019. Effects of iron oxide (Fe3O4) nanoparticles on Escherichia coli antibiotic-resistant strains. J. Appl. Microbiol. 126 (4), 1108–1116.

Gisi, U., 1996. Synergistic interaction of fungicides in mixtures. Phytopathology 86 (11), 1273–1279.

Hoseinzadeh, E., Makhdoumi, P., Taha, P., Hossini, H., Stelling, J., Kamal, M.A., Ashraf, G.M.D., 2017. A review on nano-antimicrobials: metal nanoparticles, methods and mechanisms. Curr. Drug Metab. 18 (2), 120–128.

Huang, W., Wang, C., Duan, H., Bi, Y., Wu, D., Du, J., Yu, H., 2018. Synergistic antifungal effect of biosynthesized silver nanoparticles combined with fungicides. Int. J. Agric. Biol. 20 (5), 1225–1229.

Jamdagni, P., Rana, J.S., Khatri, P., 2018. Comparative study of antifungal effect of green and chemically synthesised silver nanoparticles in combination with carbendazim, mancozeb, and thiram. IET Nanobiotechnol. 12 (8), 1102–1107.

Jampilek, J., 2016. How can we bolster the antifungal drug discovery pipeline? Future Med. Chem. 8 (12), 1393–1397.

Kah, M., Kookana, R.S., Gogos, A., Bucheli, T.D., 2018. A critical evaluation of nanopesticides and nanofertilizers against their conventional analogues. Nat. Nanotechnol. 13 (8), 677–684.

Kalampokis, I.F., Kapetanakis, G.C., Aliferis, K.A., Diallinas, G., 2018. Multiple nucleobase transporters contribute to boscalid sensitivity in aspergillus nidulans. Fungal Genet. Biol. 115, 52–63.

Kalamarakis, A.E., Petsikos-Panagiotarou, N., Mavroidis, B., Ziogas, B.N., 2000. Activity of fluazinam against strains of Botrytis cinerea resistant to benzimidazoles and/or dicarboximides and to a benzimidazole-phenylcarbamate mixture. J. Phytopathol. 148 (7–8), 449–455.

Kalia, A., Kaur, J., Tondey, M., Manchanda, P., Bindra, P., Alghuthaymi, M.A., Shami, A., Abd-Elsalam, K.A., 2021. Differential antimycotic and antioxidant potentials of chemically synthesized zinc-based nanoparticles derived from different reducing/complexing agents against pathogenic fungi of maize crop. J. Fungi 7 (3), 223. https://doi.org/10.3390/jof7030223.

Khan, S.T., Musarrat, J., Al-Khedhairy, A.A., 2016. Countering drug resistance, infectious diseases, and sepsis using metal and metal oxides nanoparticles: current status. Colloids Surf. B: Biointerfaces 146, 70–83.

Król, A., Pomastowski, P., Rafińska, K., Railean-Plugaru, V., Buszewski, B., 2017. Zinc oxide nanoparticles: synthesis, antiseptic activity and toxicity mechanism. Adv. Colloid Interf. Sci. 249, 37–52.

Kumari, M., Giri, V.P., Pandey, S., Kumar, M., Katiyar, R., Nautiyal, C.S., Mishra, A., 2019. An insight into the mechanism of antifungal activity of biogenic nanoparticles than their chemical counterparts. Pestic. Biochem. Physiol. 157, 45–52.

Leroux, P., Walker, A.-S., 2013. Activity of fungicides and modulators of membrane drug transporters in field strains of Botrytis cinerea displaying multidrug resistance. Eur. J. Plant Pathol. 135 (4), 683–693.

Li, J., Sang, H., Guo, H., Popko, J.T., He, L., White, J.C., Parkash Dhankher, O., Jung, G., Xing, B., 2017. Antifungal mechanisms of ZnO and Ag nanoparticles to Sclerotinia homoeocarpa. Nanotechnology 28 (15), 155101. https://doi.org/10.1088/1361-6528/aa61f3.

Logrieco, A., Moretti, A., Solfrizzo, M., 2009. Alternaria toxins and plant diseases: an overview of origin, occurrence and risks. World Mycotoxin J. 2, 129–140.

Malandrakis, A.A., Vattis, K.N., Markoglou, A.N., Karaoglanidis, G.S., 2017. Characterization of boscalid-resistance conferring mutations in the SdhB subunit of respiratory complex II and impact on fitness and mycotoxin production in penicillium expansum laboratory strains. Pestic. Biochem. Physiol. 138, 97–103.

Malandrakis, A.A., Apostolidou, Z.A., Louka, D., Markoglou, A., Flouri, F., 2018. Biological and molecular characterization of field isolates of Alternaria alternata with single or double resistance to respiratory complex II and III inhibitors. Eur. J. Plant Pathol. 152 (1), 199–211.

Malandrakis, A.A., Kavroulakis, N., Avramidou, M., Papadopoulou, K.K., Tsaniklidis, G., Chrysikopoulos, C.V., 2021a. Metal nanoparticles: Phytotoxicity on tomato and effect on symbiosis with the Fusarium solani FsK strain. Sci. Total Environ. 787, 147606. https://doi.org/10.1016/j.scitotenv.2021.147606.

Malandrakis, A.A., Kavroulakis, N., Chrysikopoulos, C.V., 2021b. Copper nanoparticles against benzimidazole-resistant Monilinia fructicola field isolates. Pestic. Biochem. Physiol. 173, 104796. https://doi.org/10.1016/j.pestbp.2021.104796.

Malandrakis, A.A., Kavroulakis, N., Chrysikopoulos, C.V., 2020a. Synergy between Cu-NPs and fungicides against Botrytis cinerea. Sci. Total Environ. 703, 135557. https://doi.org/10.1016/j.scitotenv.2019.135557.

Malandrakis, A.A., Kavroulakis, N., Chrysikopoulos, C.V., 2020b. Use of silver nanoparticles to counter fungicide-resistance in Monilinia fructicola. Sci. Total Environ. 747, 141287. https://doi.org/10.1016/j.scitotenv.2020.141287.

Malandrakis, A.A., Kavroulakis, N., Chrysikopoulos, C.V., 2019. Use of copper, silver and zinc nanoparticles against foliar and soil-borne plant pathogens. Sci. Total Environ. 670, 292–299.

Márquez, I.G., Ghiyasvand, M., Massarsky, A., Babu, M., Samanfar, B., Omidi, K., Moon, T.W., Smith, M.L., Golshani, A., 2018. Zinc oxide and silver nanoparticles toxicity in the baker's yeast, Saccharomyces cerevisiae. PLoS ONE 13 (3), e0193111. https://doi.org/10.1371/journal.pone.019311.

Markoglou, A.N., Malandrakis, A.A., Vitoratos, A.G., Ziogas, B.N., 2006. Characterization of laboratory mutants of Botrytis cinerea resistant to QoI fungicides. Eur. J. Plant Pathol. 115 (2), 149–162.

Morris, P.F., Connolly, M.S., St Clair, D.A., 2000. Genetic diversity of Alternaria alternata isolated from tomato in California assessed using RAPDs. Mycol. Res. 104, 286–292.

Nejabatdoust, A., Salehzadeh, A., Zamani, H., Moradi-Shoeili, Z., 2019. Synthesis, characterization and functionalization of ZnO nanoparticles by glutamic acid (Glu) and conjugation of ZnO@Glu by thiosemicarbazide and its synergistic activity with ciprofloxacin against multi-drug resistant Staphylococcus aureus. J. Clust. Sci. 30 (2), 329–336.

Nisar, P., Ali, N., Rahman, L., Ali, M., Shinwari, Z.K., 2019. Antimicrobial activities of biologically synthesized metal nanoparticles: an insight into the mechanism of action. J. Biol. Inorg. Chem. 24 (7), 929–941.

Pandey, S., Giri, K., Kumar, R., Mishra, G., Raja Rishi, R., 2018. Nanopesticides: opportunities in crop protection and associated environmental risks. Proc. Natl. Acad. Sci. India B Biol. Sci. 88 (4), 1287–1308.

Paralikar, P., Ingle, A.P., Tiwari, V., Golinska, P., Dahm, H., Rai, M., 2019. Evaluation of antibacterial efficacy of sulfur nanoparticles alone and in combination with antibiotics against multidrug-resistant uropathogenic bacteria. J. Environ. Sci. Health A Tox. Hazard. Subst. Environ. Eng. 54 (5), 381–390.

Priyadarshini, E., Priyadarshini, S.S., Cousins, B.G., Pradhan, N., 2021. Metal-Fungus interaction: review on cellular processes underlying heavy metal detoxification and synthesis of metal nanoparticles. Chemosphere 274, 129976. https://doi.org/10.1016/j.chemosphere.2021.129976.

Punjabi, K., Mehta, S., Chavan, R., Chitalia, V., Deogharkar, D., Deshpande, S., 2018. Efficiency of biosynthesized silver and zinc nanoparticles against multi-drug resistant pathogens. Front. Microbiol. 9 (SEP), 2207. https://doi.org/10.3389/fmicb.2018.02207.

Rai, M., Ingle, A.P., Pandit, R., Paralikar, P., Gupta, I., Chaud, M.V., dos Santos, C.A., 2017. Broadening the spectrum of small-molecule antibacterials by metallic nanoparticles to overcome microbial resistance. Int. J. Pharm. 532 (1), 139–148.

Robinson, J.R., Isikhuemhen, O.S., Anike, F.N., 2021. Fungal–metal interactions: a review of toxicity and homeostasis. J. Fungi 7 (3), 225. https://doi.org/10.3390/jof7030225.

Ruddaraju, L.K., Pammi, S.V.N., Guntuku, G.S., Padavala, V.S., Kolapalli, V.R.M., 2020. A review on anti-bacterials to combat resistance: from ancient era of plants and metals to present and future perspectives of green nano technological combinations. Asian J. Pharm. Sci. 15 (1), 42–59.

Rudramurthy, G.R., Swamy, M.K., Sinniah, U.R., Ghasemzadeh, A., 2016. Nanoparticles: alternatives against drug-resistant pathogenic microbes. Molecules 21 (7), 836. https://doi.org/10.3390/molecules21070836.

Sang, H., Lee, H.B., 2020. Molecular mechanisms of succinate dehydrogenase inhibitor resistance in phytopathogenic Fungi. Res. Plant Dis. 26 (1), 1–7.

Sardella, D., Gatt, R., Valdramidis, V.P., 2017. Physiological effects and mode of action of ZnO nanoparticles against postharvest fungal contaminants. Food Res. Int. 101, 274–279. https://doi.org/10.1016/j.foodres.2017.08.019.

Sierotzki, H., Scalliet, G., 2013. A review of current knowledge of resistance aspects for the next-generation succinate dehydrogenase inhibitor fungicides. Phytopathology 103, 880–887.

Slavin, Y.N., Asnis, J., Häfeli, U.O., Bach, H., 2017. Metal nanoparticles: understanding the mechanisms behind antibacterial activity. J. Nanobiotechnol. 15 (1), 65. https://doi.org/10.1186/s12951-017-0308-z.

Strandberg, J.O., 1992. Alternaria species that attack vegetable crops: biology and options for disease management. In: Chelkowski, J., Visconti, A. (Eds.), Alternaria Biology, Plant Diseases, and Metabolites, Topics in Secondary Metabolism. 3. Elsevier Science Publishers B. V, Amsterdam, pp. 175–208.

Sun, Q., Li, J., Le, T., 2018. Zinc oxide nanoparticle as a novel class of antifungal agents: current advances and future perspectives. J. Agric. Food Chem. 66 (43), 11209–11220.

Sun, L., Liao, K., Li, Y., Zhao, L., Liang, S., Guo, D., Hu, J., Wang, D., 2016. Synergy between polyvinylpyrrolidone-coated silver nanoparticles and azole antifungal against drug-resistant Candida albicans. J. Nanosci. Nanotechnol. 16 (3), 2325–2335.

Veloukas, T., Markoglou, A.N., Karaoglanidis, G.S., 2013. Differential effect of SdhB gene mutations on the sensitivity to SDHI fungicides in Botrytis cinerea. Plant Dis. 97, 118–122.

Xiao, C.L., Boal, R.J., 2009. Preharvest application of a boscalid and pyraclostrobin mixture to control postharvest graymold and blue mold in apples. Plant Dis. 93, 185–189.

Xue, J., Luo, Z., Li, P., Ding, Y., Cui, Y., Wu, Q., 2014. A residue-free green synergistic antifungal nanotechnology for pesticide thiram by ZnO nanoparticles. Sci. Rep. 4, 5408. https://doi.org/10.1038/srep05408.